

SHORTER COMMUNICATIONS

NON-DARCY NATURAL CONVECTION FROM HEATED SURFACES IN SATURATED POROUS MEDIA

O. A. PLUMB* and J. C. HUENEFELD†

Department of Mechanical Engineering, Washington State University, Pullman, WA 99164, U.S.A.

(Received 31 March 1980 and in revised form 19 August 1980)

NOMENCLATURE

D_p	pore or particle diameter;
f	dimensionless stream function;
g	acceleration of gravity;
Gr'	modified Grashof number, $g\beta K K' (t_w - t_\infty)/\nu^2$;
J	hydraulic gradient;
K	permeability;
K'	inertial coefficient in the Ergun equation;
Nu_{xx}	local Nusselt number;
n	power law dependence of surface temperature;
p	pressure;
Ra_{xx}	Rayleigh number, $g\beta K x(t_w - t_\infty)/\nu\alpha$;
t	temperature;
t_w	surface temperature;
t_∞	ambient fluid temperature;
u	streamwise specific discharge;
v	cross stream specific discharge;
x	streamwise coordinate;
y	cross stream coordinate.

Greek symbols

α	effective thermal diffusivity of saturated porous medium;
β	coefficient of thermal expansion;
ε	porosity;
η	independent similarity variable;
θ	dimensionless temperature;
μ	molecular viscosity;
ν	kinematic viscosity;
ρ	fluid density;
ψ	stream function.

INTRODUCTION

NATURAL convection in saturated porous media has recently received considerable attention because of numerous applications in geophysics and energy related engineering problems. Such applications include natural circulation in geothermal reservoirs, aquifers, porous insulations, packed bed reactors, sensible heat storage beds, and beds of fossil fuels such as oil shale and coal which have been fragmented for *in situ* energy extraction.

Several buoyancy driven boundary layer flows have been analyzed by Cheng and Minkowycz and their associates [1-7] for the case of a Darcy flow. However, the non-Darcy flow situation which may prevail in some of the above applications has not been considered. In this paper the buoyancy induced boundary layer adjacent to a vertical heated surface is analyzed using a non-Darcy flow model. In addition, the extension of the analysis to other geometries is

considered. For the case of a vertical isothermal surface similarity exists under the assumed conditions and, thus, the governing partial differential equations are reduced to a set of ordinary differential equations. For the more general case of a power law variation in surface temperature the flow is non-similar.

THE NON-DARCY FLOW MODEL

A detailed discussion of the limitations of Darcy's law and non-Darcy flow models is presented by Bear [8]. Deviations from Darcy's law are known to occur when the Reynolds number based on the mean pore diameter exceeds 1 to 10. This deviation can be attributed to inertial forces which are negligible in comparison to viscous forces for Reynolds numbers less than unity. The earliest non-Darcy flow model is that proposed by Forchheimer [9] which can be written in one dimension as follows:

$$Au + Bu^2 = J \quad (1)$$

where J is the hydraulic gradient, u is the specific discharge and A and B are empirical constants which must be determined from experiment. Since Forchheimer's pioneering studies numerous non-Darcy flow models have been proposed, most of which take the same general form as equation (1). The primary advantage of the more recent models is that the constant A and B are completely specified in terms of the properties of the fluid and the porous medium. Such models include those developed by Ergun [10], Schneebeli [11], Ward [12], and Irmay [13], among others. The Ergun model will be used in the forthcoming analysis, however, the results are valid for any of the models through adjustment of the transport properties which appear in the governing equations.

The Ergun equation can be written (in one-dimension) as

$$\left[\frac{150(1-\varepsilon)^2 \mu}{D_p^2 \varepsilon^3} \right] u + \frac{1.75(1-\varepsilon)}{D_p \varepsilon^3} \rho u^2 = J \quad (2)$$

which is the same form as (1) except the empirical constants A and B have been expressed in terms of fluid and medium properties. Equation (2) can be written as follows by lumping the medium properties into a single coefficient:

$$u + \frac{\rho}{\mu} K' u^2 = -\frac{K}{\mu} \frac{\partial p}{\partial x} \quad (3)$$

where

$$K = \frac{D_p^2 \varepsilon^3}{150(1-\varepsilon)^2} \quad (4)$$

is recognized as the permeability expressed in terms of a characteristic pore or particle diameter and the porosity, and

$$K' = \frac{1.75 D_p}{150(1-\varepsilon)} \quad (5)$$

* Assistant Professor

† Graduate Student

is the transport property related to the inertial effect. As $K' \rightarrow 0$ equation (3) reduces to Darcy's law. The major difference between the Ergun model and others is in the explicit dependence of K and K' on the properties of the medium.

ANALYSIS

If we assume a two-dimensional flow with constant fluid and medium (isotropic) properties, local thermodynamic equilibrium between fluid and solid phases and invoke the Boussinesq approximation, the governing equations can be written

$$\frac{\partial u}{\partial x} + \frac{\partial v}{\partial y} = 0 \tag{6}$$

$$u + \frac{\rho u^2 K'}{\mu} = -\frac{K}{\mu} \left[\frac{\partial p}{\partial x} - \rho g \beta (t - t_\infty) \right] \tag{7}$$

$$v + \frac{\rho v^2}{\mu} \quad K' = -\frac{K}{\mu} \frac{\partial p}{\partial y} \tag{8}$$

$$u \frac{\partial t}{\partial x} + v \frac{\partial t}{\partial y} = \alpha \frac{\partial^2 t}{\partial y^2} \tag{9}$$

Here the boundary-layer approximation has been invoked with regard to the energy equation and α is the effective thermal diffusivity of the fluid-solid system. The boundary conditions to be considered are

at

$$\begin{aligned} y = 0: \quad v = 0 \quad t_w = t_\infty + Ax^n \\ y \rightarrow \infty: \quad u = 0 \quad t = t_\infty. \end{aligned} \tag{10}$$

Upon introduction of the stream function,

$$u = \frac{\partial \psi}{\partial y}, \quad v = -\frac{\partial \psi}{\partial x} \tag{11}$$

cross differentiating (7) and (8) to eliminate pressure, and invoking the boundary-layer approximation with regard to the equation for the stream function ($\partial^2 \psi / \partial x^2 \ll \partial^2 \psi / \partial y^2$ and $\partial \psi / \partial x \ll \partial \psi / \partial y$) the resulting equations can be written

$$\frac{\partial^2 \psi}{\partial y^2} + \frac{K'}{v} \frac{\partial}{\partial y} \left(\frac{\partial \psi}{\partial y} \right)^2 = \frac{g \beta K}{v} \frac{\partial t}{\partial y} \tag{12}$$

$$\frac{\partial \psi}{\partial y} \frac{\partial t}{\partial x} - \frac{\partial \psi}{\partial x} \frac{\partial t}{\partial y} = \alpha \frac{\partial^2 t}{\partial y^2} \tag{13}$$

The boundary-layer approximation leads to retention of the inertial term only in the streamwise direction.

Equations (13) and (14) along with the appropriate boundary conditions can be transformed to the similarity coordinates introduced by Cheng and Minkowycz [1].

$$\begin{aligned} \eta &= \frac{y}{x} (Ra_x)^{1/2} \\ \psi &= \alpha (Ra_x)^{1/2} f(\eta) \\ \theta &= \frac{t - t_\infty}{t_w - t_\infty} \end{aligned} \tag{14}$$

where

$$Ra_x = \frac{g \beta K}{\nu \alpha} (t_w - t_\infty) x$$

resulting in the following equations:

$$f'' + \frac{g \beta K K' (t_w - t_\infty)}{\nu^2} (f')^2 - \theta' = 0 \tag{15}$$

$$\theta'' + \left(\frac{n+1}{2} \right) f' \theta' - n f' \theta = 0 \tag{16}$$

with boundary conditions

at

$$\begin{aligned} \eta = 0: \quad f = 0, \quad \theta = 1 \\ \eta \rightarrow \infty: \quad f' = 0, \quad \theta = 0. \end{aligned} \tag{17}$$

It can be seen that similarity is admitted by (15) only for the case of an isothermal surface ($n = 0$) in which case

$$f'' + Gr'(f')^2 - \theta' = 0 \tag{18}$$

$$\theta'' + 1/2 f \theta' = 0 \tag{19}$$

where

$$Gr' = \frac{g \beta K K' (t_w - t_\infty)}{\nu^2} \tag{20}$$

is a modified Grashof number expressing the relative importance of the inertial effects.

Several other cases examined by Cheng and coworkers which lead to similarity for Darcy flow are also similar when the non-Darcy effect is included. These include free convection about isothermal inclined plates where the normal component of the acceleration of gravity can be neglected [7], mixed convection about a vertical isothermal surface [5], mixed convection on a horizontal surface with temperature increasing as $x^{1/2}$ in the streamwise direction [6] and natural convection from vertical isothermal cylinders [2].

RESULTS AND DISCUSSION

Numerical solutions to the equations (18) and (19) for the vertical isothermal surface were obtained. Since similarity results for the isothermal surface, the solution is a relatively routine numerical integration of the equations using a fourth order predictor-corrector routine.

The resulting profiles of dimensionless streamwise velocity and temperature for the isothermal case are shown in Figs. 1 and 2 as a function of the parameter Gr' . As can be seen in the figures, the inertial term begins to have a pronounced effect on the flow for values of $Gr' > 0.1$. As Gr' is increased beyond this point, the velocity peak which occurs (in theory) at the wall decreases and both the thermal and velocity boundary layers become thicker. The end result is, thus, a decrease in the heat transfer.

The local Nusselt number is given by the relationship

$$Nu_x = -\theta'(0) (Ra_x)^{1/2} \tag{21}$$

For $Gr' = 0$ which implies Darcy flow $-\theta'(0)$ was computed to be 0.44390 as compared to 0.4440 reported in [1]. The rate of $\theta'(0)$ for the non-Darcy case to that for the Darcy case (designated $\theta'_0(0)$) is shown in Fig. 3 for values of Gr' ranging

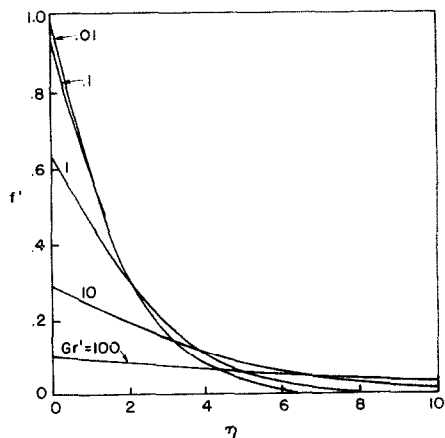


FIG. 1. Dimensionless velocity distribution as a function of the parameter, Gr' .

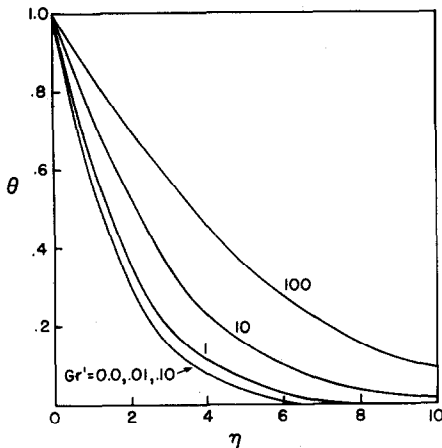


FIG. 2. Dimensionless temperature as a function of the parameter, Gr' .

from 0.01 to 100. Tabulated values of $\theta'(0)$ and $f'(0)$ are given in Table 1. For values of Gr' up to 0.1, the heat transfer deviates from the Darcy case by less than 5% but drops off rapidly as Gr' is increased beyond 0.1.

Table 1. Dimensionless temperature and velocity gradients at $\eta = 0$

Gr'	Isothermal $\theta'(0)$	$f'(0)$
0.00	-0.44390	1.00000
0.01	-0.44232	0.99020
0.10	-0.42969	0.91608
1.00	-0.36617	0.61803
10.00	-0.25126	0.27016
100.00	-0.15186	0.09512

The results demonstrate that the relative importance of the inertial effects is characterized by the modified Grashof number, Gr' , defined in equation (21). For vertical heated surfaces the deviation of the heat transfer from that for Darcy flow is less than 5% for $Gr' < 0.1$. For $Gr' > 0.1$ the deviation increases rapidly and inertial effects should be incorporated in the analysis.

Acknowledgements—This research was supported in part by the National Science Foundation under Grant No. ENG-7820145.

REFERENCES

1. P. Cheng and W. J. Minkowycz, Free convection about a vertical flat plate imbedded in a porous medium with application to heat transfer from a dike, *J. Geophys. Res.* **82**, 2040-2044 (1977).
2. W. J. Minkowycz and P. Cheng, Free convection about a vertical cylinder imbedded in a porous medium, *Int. J. Heat Mass Transfer* **19**, 805-813 (1976).
3. P. Cheng and I-Dee Chang, Buoyancy induced flow in a saturated porous media adjacent to impermeable horizontal surface, *Int. J. Heat Mass Transfer* **19**, 1267-1272 (1976).
4. P. Cheng, The influence of lateral mass efflux on free convection boundary layers in a saturated porous medium, *Int. J. Heat Mass Transfer* **20**, 201-206 (1977).
5. P. Cheng, Combined free and forced boundary layer flows about inclined surfaces in a porous medium, *Int. J. Heat Mass Transfer* **20**, 806-814 (1977).
6. P. Cheng, Similarity solutions for mixed convection from horizontal impermeable surfaces in saturated porous media, *Int. J. Heat Mass Transfer* **20**, 893-898 (1977).
7. C. H. Johnson and P. Cheng, Possible similarity solutions for free convection boundary layers adjacent to flat plates in porous media, *Int. J. Heat Mass Transfer* **21**, 669-676 (1978).
8. J. Bear, *Dynamics of Fluids in Porous Media*. Elsevier, New York (1972).
9. P. Forchheimer, Wasserbewegung durch Boden, *Fortschrift Ver. D. Ing.* **45**, 1782-1788 (1901).

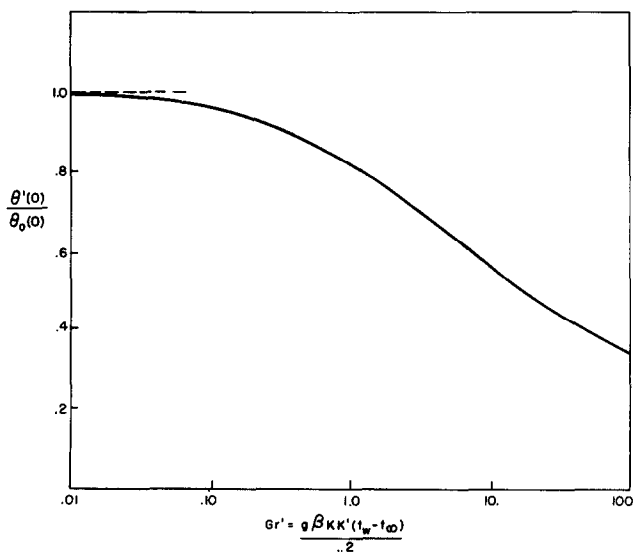


FIG. 3. The ratio of heat transfer with inertial effects to that with no inertial effects as a function of the parameter, Gr' .

10. S. Ergun, Fluid flow through packed columns, *Chem. Engng Prog.* **48**, 89–94 (1952).
11. G. Schneebeli, Experiences sur la limite de validite de la loi de Darcy et l'apparition de la turbulence dan un ecoulement de filtration, *Huile Blanche No. 2*, **10**, 141–149 (1955).
12. J. C. Ward, Turbulent flow in porous media, *Proc. Am. Soc. Civ. Engng No. HY5* **90**, 1–12 (1969).
13. S. Irmay, Theoretical models of flow through porous media, *R.I.L.E.M. Symp. Transfer of Water in Porous Media*, Paris (1964).

Int. J. Heat Mass Transfer. Vol. 24, No. 4, pp. 768–770, 1981
Printed in Great Britain

0017-9310/81/040768-03 \$02.00/0
Pergamon Press Ltd

THE EFFECT OF SUBCHANNEL SHAPE ON HEAT TRANSFER IN ROD BUNDLES WITH AXIAL FLOW

W. J. SEALE

School of Mechanical Engineering, University of Bradford, Bradford BD7 1DP, U.K.

(Received 12 February 1980 and in revised form 11 July 1980)

NOMENCLATURE

A ,	anisotropy factor, K_p/K_r , equation (1);
b ,	gap width between adjacent rods;
C_p ,	specific heat at constant pressure;
d ,	rod diameter;
d_e ,	subchannel equivalent diameter = $4F/S$;
F ,	flow area of subchannel;
h ,	duct height, Fig. 1;
k ,	turbulence kinetic energy;
K_p ,	effective conductivity parallel to surface;
K_r ,	effective conductivity normal to surface;
p ,	rod pitch;
Q ,	heat transfer/unit length between adjacent subchannels;
Re ,	subchannel Reynolds number, $\rho U d_e/\mu$;
S ,	wetted perimeter;
Stg ,	gap Stanton number, $Q/b(T_i - T_j)\rho U C_p$;
T_i, T_j ,	bulk mean temperatures in adjacent subchannels, Fig. 1;
U ,	mean axial velocity;
y ,	normal distance from wall;
\hat{y} ,	normal distance from wall to surface of no-shear,
Y ,	mixing factor, equation (3).

Greek symbols

ϵ ,	dissipation of turbulence kinetic energy;
μ ,	dynamic viscosity, evaluated at bulk mean temperature;
ρ ,	density, evaluated at bulk mean temperature.

INTRODUCTION

IN THE rod bundle of a nuclear reactor the heat transfer across the narrow gaps between the fuel rods is considerably higher than predicted by isotropic turbulent diffusion theory, and is relatively independent of gap width [1]. Work reported earlier [1, 2] showed that these phenomena were caused by a substantial anisotropy of the effective conductivity: the value in the direction through the gap, parallel to the rod surface, was much higher than the value normal to the surface. Turbulence driven secondary flows were found to be unimportant.

Much of the experimental data on inter-subchannel heat transfer has been reduced to simple correlations by Rogers and Rosehart [3], and Ingesson and Hedberg [4], and these show that the heat transfer rate through the gaps is strongly influenced by the shape of the adjacent subchannels as characterized by the ratios p/d and p/d_e . To investigate the effect of subchannel shape on the inter-subchannel heat flow the earlier theoretical analysis [2] has been extended to predict gap Stanton numbers in ten different subchannel geometries for three of which experimental data is available [1].

The basic shape of the adjacent subchannels is shown in Fig. 1 together with the boundary conditions; details of the ten geometries are given in Table 1. For each geometry the adjacent subchannels remain symmetrical to one another. It should be noted that the geometries 1b, 2a and 3a simulate an infinite square array, and the experimental results were obtained for geometries 1b, 2b and 3b. All surfaces were smooth, the flow was fully developed both thermally and hydraulically, and the fluid was atmospheric air.

In the earlier work it was found that the measured velocity

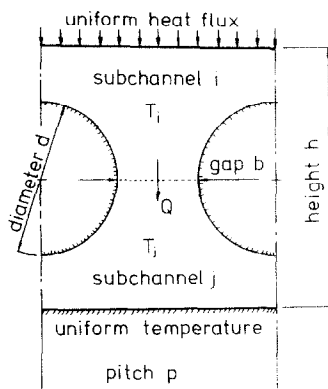


FIG. 1. Geometry investigated including thermal boundary conditions (all surfaces adiabatic except upper and lower flat walls).